Simulation and experimental evaluation on a skyhook policy-based fuzzy logic control for semi-active suspension system

Ubaidillah*

Department of Mechatronics Engineering,
Electronic Engineering Polytechnic Institute of Surabaya (EEPIS),
Jl. Raya ITS, Sukolilo, Surabaya 60111, Indonesia
E-mail: ubaid.ubaidillah@gmail.com
*Corresponding author

Khisbullah Hudha

Faculty of Mechanical Engineering,
Universiti Teknikal Malaysia Melaka (UTeM),
Ayer Keroh, 75450 Melaka, Malaysia
E-mail: khisbullah@utem.edu.my

Hishamuddin Jamaluddin

Faculty of Mechanical Engineering,
Universiti Teknologi Malaysia (UTM),
81310 UTM Skudai, Johor, Malaysia
E-mail: hishamj@fkm.utm.my

Abstract: This paper focuses on performance evaluation of several outer loop controller designs employed in a quarter car suspension featuring a magnetorheological fluid damper. A Magne-Ride damper was employed and its behaviour was investigated in the form of force-displacement and force-velocity characteristics. The non-linear hysteretic behaviour of the damper was modelled using a sixth order polynomial model. Force tracking control was performed to check the force tracking ability of the damper using a PI control. The governing equations of motions were formulated and integrated with skyhook control. Skyhook policy was then adapted in the development of a fuzzy logic control to enhance the ride performance. The performance of fuzzy logic control was compared with the on-off and continuous skyhook control in time domain. The results show that skyhook algorithm-based fuzzy logic control gives better performances than its counterparts.

Keywords: non-parametric technique; force tracking; skyhook; fuzzy logic; semi-active suspension; quarter car suspension.

Reference to this paper should be made as follows: Ubaidillah, Hudha, K. and Jamaluddin, H. (2011) 'Simulation and experimental evaluation on a skyhook policy-based fuzzy logic control for semi-active suspension system', *Int. J. Structural Engineering*, Vol. 2, No. 3, pp.243–272.

Biographical notes: Ubaidillah received his BEng in Mechanical Engineering from Institut Teknologi Sepuluh Nopember (ITS) Surabaya, Indonesia. Currently, he is a Research Assistant and a Master Student in Autotronic Laboratory, Faculty of Mechanical Engineering, Universiti Teknikal Malaysia Melaka (UTeM). His research project lies on magnetorheological fluid devices such as MR damper, MR brake and MR engine mounting for vehicle application. He is currently a Teaching Staff at the Electronic Engineering Polytechnic Institute of Surabaya (EEPIS/PENS).

Khisbullah Hudha received his BEng of Mechanical Design from the Institut Teknologi Bandung (ITB) Indonesia, MSc from the Department of Engineering Production Design, Technische Hoogeschool Utrecht, the Netherlands, and his PhD on Intelligent Vehicle Dynamics Control Using Magnetorheological Damper from Malaysia University of Technology (UTM). His research interests include modelling, identification and force tracking control of semi-active damper, evaluation of vehicle ride and handling, electronic chassis control system design and intelligent control. He is currently attached with the Universiti Teknikal Malaysia Melaka (UTeM). His profile can be reached at http://www.utem.edu.my/fkm/smac/index.htm.

Hishamuddin Jamaluddin received his BSc, MSc and PhD from the Department of Control Engineering, Sheffield University, UK. He is currently a Professor in the Department of Applied Mechanics, Faculty of Mechanical Engineering, Universiti Teknologi Malaysia, Johor, Malaysia. His research interests include non-linear system modelling, system identification, neural networks, adaptive fuzzy models, genetic algorithm, neuro-fuzzy and active force control. His profile can be reached at http://www.fkm.utm.my/~hishamj.

1 Introduction

Dynamic performances of vehicle and suspension system design have been the major focus of automobile industry for nearly a century. It is well-known that vehicle performance can be quantified in many methods. Ride comfort and good handling are two performance aspects which are directly related to the vehicle suspension system. Since the development of the vehicle suspension system, designers faced with the problem of fulfilling these two requirements simultaneously which is impossible thus the need for compromise. The trade-off is the use of single optimal adjustment of a passive damper (Carter, 1998; Yu et al., 2006). Generally, vehicles achieving good ride quality are characterised by suspension with low spring rates, low damping rates, resulting in a large suspension travel. Vehicles exhibiting good handing generally incorporate suspensions with high spring and damping rates, resulting in a small working travel (Craft et al., 2003).

Majority of cars available in the market today use passive suspension system. In more recent years, the refinement of passive suspension system in modern automobiles has resulted in acceptable levels of both handling and ride quality under common road conditions. These systems are not typically optimised for any particular type of terrain (Kazuoka, 1992). Passive suspension performance characteristics still represent a major compromise between ride quality, handling, suspension working space and maintaining body motion (Craft et al., 2003; Hennecke and Zeiglmeier, 1988). It offers only limited

option when compared to the controllable suspensions system such as semi-active and fully active systems.

Research focused on reducing unwanted vibration in the vehicle has led to the development of computer-controlled suspension system and also to the development of numerous damper control policies (Gillespie, 1992). Active suspension system is achieved through the application of controlled external force usually applied between the sprung and unsprung masses of each wheel assembly. The force can be provided by pneumatics, hydraulics or electromechanical actuators (Hudha et al., 2008). Therefore, the active suspension system incorporates extra energy source, cost and the weight to refine the compromise. It generally requires high energy and the system could be unstable in case of power failure (Singla and Singh, 2004; Buckner et al., 2000). Early 1974, Karnop et al. (1974) also realised the potential disadvantages associated with active control implementations, in terms of cost, complexity, power consumption and response time.

For these reasons, many researchers pay more attention on semi-active suspension system. Semi-active suspension system offers substantially better performance than passive suspension system. While it cannot offer the full benefits compared with active suspension system. Two types of semi-active suspension systems have been developed, namely variable orifice damper and variable fluid viscosity damper. Recent developments in variable fluid viscosity damper have made it a feasible mean of implementing semi-active suspension. The wide viscosity range associated with electrorheological (ER) and magnetorheological (MR) fluids combined with their high bandwidths make them excellent choices for use in semi-active devices (Carlson, 2001). However, ER fluids require high control voltages, cannot produce high shear force and are susceptible to contaminants, therefore ER fluids are not ideally suitable for automotive applications (Jolly et al., 1998). Compared with ER fluids, MR fluids produce large shear forces in the presence of magnetic fields (Craft et al., 2003). MR fluids also require lower excitation power and are easily adopted for use in automotive components.

Semi-active suspensions have been shown to offer valuable benefits for vehicle primary suspension. Moreover, semi-active suspension systems have developed into a technology that is currently being implemented (Ahmadian and Goncalves, 2004). Available in the year 2002, Cadillac Seville STS uses an MR damper made by Delphi to vary the damping according to the driving conditions (Hudha et al., 2005). Maserati also offers a semi-active suspension that implemented newly developed Mannesmann Sachs skyhook control system in its 2002 Spyder (Hutton, 2001). Semi-active control strategy was firstly introduced by Karnopp and Crosby (1973). One is the semi-active 'on-off' system, in which hard and soft damping coefficients are switched depending on the sign of the product of body velocity and damper relative velocity. The other control scheme is the continuous skyhook system which is based on the skyhook theory (Motta et al., 2000).

This paper presents the study where a type of MR damper was tested and its hysteresis behaviour was investigated based on experimental and simulation works. The experimental results are evaluated in terms of the damping force versus piston velocity and the damping force versus piston displacement. A polynomial approach is used to model the MR damper namely a sixth order polynomial model, which is a class of non-parametric technique. In addition, the accuracy of the damping force control using the proposed model is demonstrated in both simulation and experimental studies by employing a simple closed-loop PI control. The inner loop control was simulated to

check the tracking ability of the MR damper by employing the validated MR damper model under several input functions such as sinusoidal, square, and saw-tooth. The experimental investigation of the force tracking control was conducted using several sinusoidal input frequencies and amplitudes of the desired damping forces.

Semi-active control algorithms, namely 'On-off' skyhook and continuous skyhook were used with an MR damper and were evaluated in time domain simulation using a sinusoidal road input. Then, a fuzzy logic control was developed based on continuous skyhook algorithm. The performance of the fuzzy logic control was investigated through simulation study and experimental work. Both 'on-off' skyhook and continuous skyhook control results are used as a benchmark for the fuzzy logic control. The experimental work was conducted on a linear quarter car test rig using sinusoidal road input. This is due to the limitation of the quarter car test rig available at the department of Automotive, UTeM.

This paper is organised as follows: the first section contains introduction on semi-active MR fluids damper and review of the previous works on related field, the second section explains the behaviour of MR damper in the form of force-velocity and force-displacement characteristics, the third section describes the approach of MR damper modelling, the fourth section explains the controller architecture used in this study that consists of inner loop and outer loop controller, the fifth section contains the hardware implementation and experimental setup, the sixth section presents the simulation results and performance evaluation for different types of control techniques, the seventh section discusses the experimental results and the last section presents the conclusions.

2 MR damper force behaviour

A passive viscous damper contains fluid that helps the mechanical structure to dissipate energy and mitigate vibration response. In particular, an MR damper is filled with a controllable fluid that contains dispersed micron-sized magnetically polarisable particles. When the fluid is subjected to magnetic field, the particles are arranged in a pattern and the behaviour of the fluid is changed from being linear viscous to semi-solid in milliseconds. By adjusting the current within an allowable range, the resisting force to motion of the MR damper increases or decreases in a non-linear fashion. When various magnitudes and patterns of current are applied to the MR damper, resistance of the damper to motion can be adjusted. A schematic of a typical MR damper is illustrated in Figure 1.

Figure 1 Schematic of an MR damper

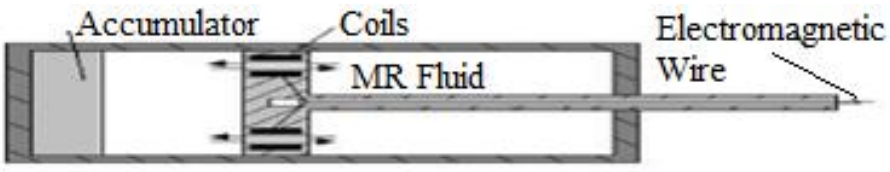

Since the proposed damper model depends on the availability of experimental data, the experimental investigation of force-velocity and force-displacement characteristics of the

MR damper needs to be performed. Experiments were set up to obtain the data for identification of the proposed the MR damper model first. Based on the experimental data, a modelling method of the MR damper was realised numerically using a sixth order polynomial equation.

The MR damper used in this study is a Magne-Ride Delphi, which was manufactured by Delphi Automotive System. The damper consists of a monotube house, piston, magnetic circuit, accumulator, and pressurised gas inside an accumulator and MR fluid. The length of the damper is 48 cm in its extended position and has 8 cm of stroke. The maximum current applied to the electromagnet coils in the magnetic choke is 3.5 Amp and the coil resistance is 1.6 Ohm.

The experimental work was carried out in the Autotronic Laboratory, Department of Automotive, Universiti Teknikal Malaysia Melaka (UTeM) using a shock absorber test machine developed by the Smart Material and Automotive Control Group, UTeM. The shock absorber test machine consists of a wire transducer to measure the relative displacement and relative velocity of the damper and load cell to measure the damper force. The Integrated Measurement and Control (IMC) device provides signal processing of the transducers and excitation signals of the slider crank actuator system. These signals are digitally processed and stored in a personal computer using FAMOS control software (IMC, 2002). IMC device is connected to the personal computer using NetBEUI protocol (Scholz, 2000). Control signals to the MR damper are converted to analogue signals by the IMC device. Then, the voltage signals are passed through the current driver and sent to the MR damper. The configuration of the shock absorber test machine available in Autotronic Laboratory is shown in Figure 2.

Figure 2 Shock absorber test machine available at Autotronic Laboratory

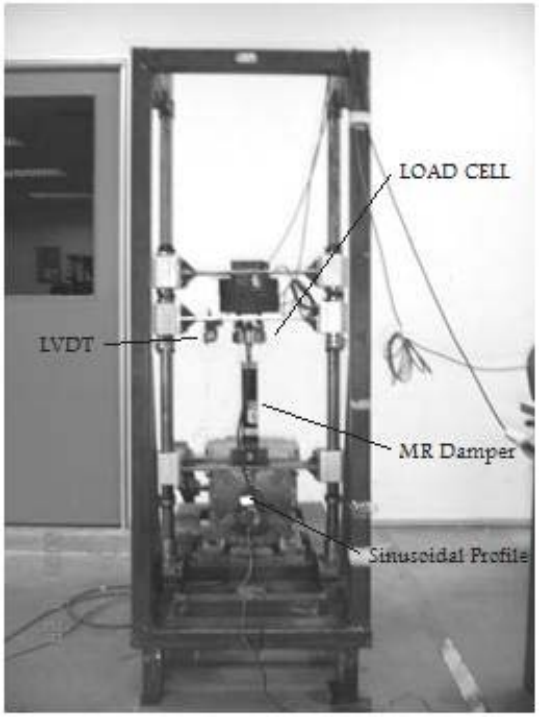

Figure 3 Measured forces for five constant current levels

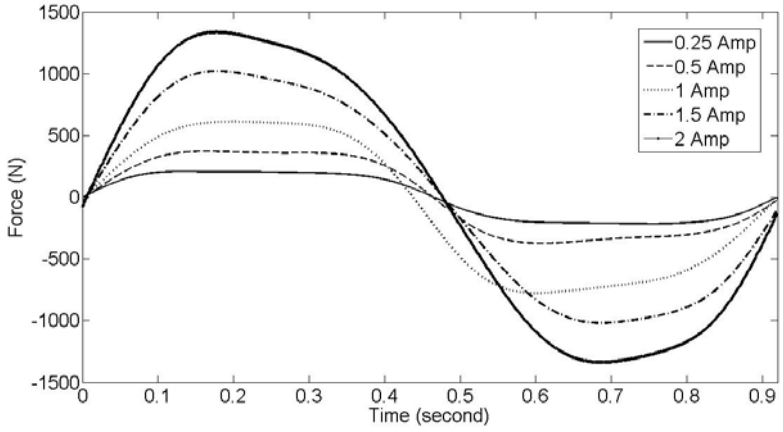

Figure 4 Force-velocity characteristic for five constant current levels

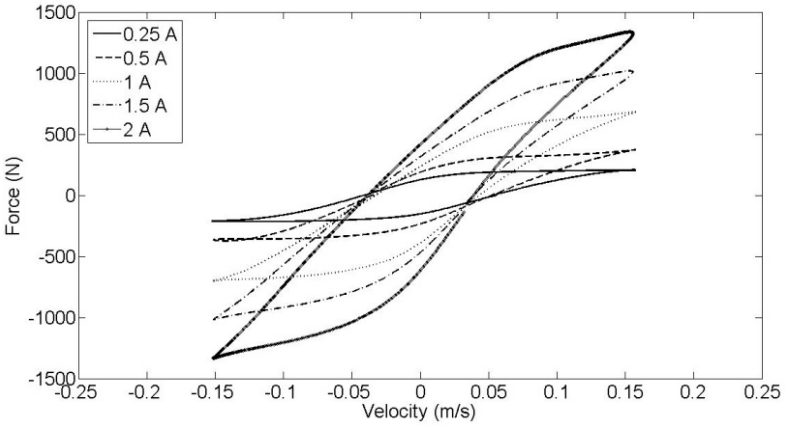

Figure 5 Force-displacement characteristic for five constant current levels

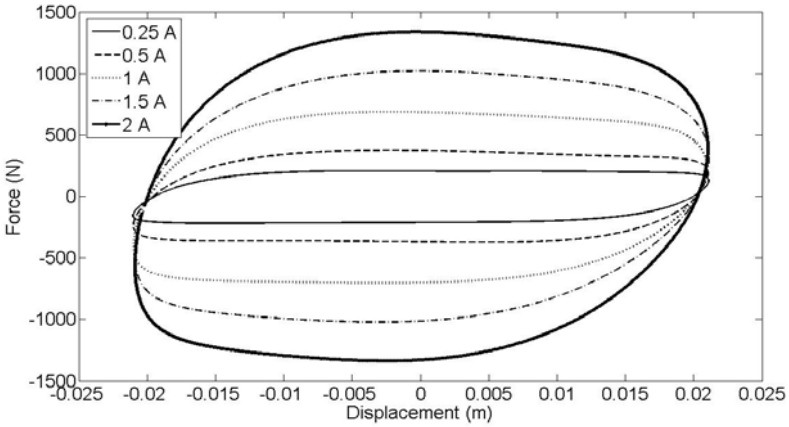

The MR damper testing was done by applying a cyclic motion between the upper and lower ends of the MR damper for different values of applied currents to the damper coils. The response of the MR damper due to 1.08 Hz sinusoidal excitation with amplitude of 2.1 cm was investigated for five constant currents of 0.25, 0.5, 1, 1.5 and 2 Ampere, being applied by the current driver of the MR damper. The measured forces in time domain, the force-velocity characteristics and the force-displacement characteristics are shown in Figures 3, 4 and 5 respectively. It can be seen from Figures 4 and 5 that the magnitude of the damping force at the piston velocity and displacement increases proportionally with the increase of the current applied to the damper coils.

Figure 6 The structure of the sixth order polynomial model

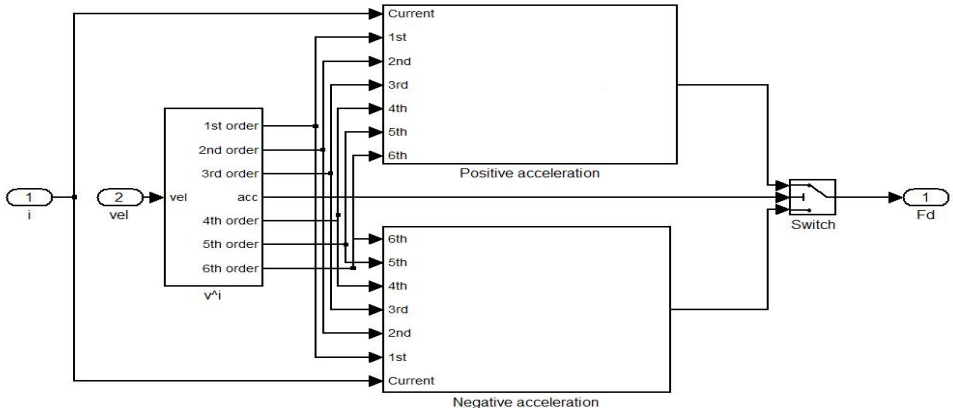

3 MR damper modelling

In this work, a sixth order polynomial model proposed by Choi et al. (2001) was adopted to predict the field-dependent damping force characteristic of the damper. It is a class of non-parametric techniques which employs analytical formulation to describe the characteristics of the device based on experimental data analysis. In order to build an easy-for-implementation MR damper model for both simulation and real-time control systems, the proposed modelling approach was developed based on experimental data and consists of five main steps. The structure of the proposed MR damper model depicted by a Simulink block diagram is shown in Figure 6. In the first step, experimental works on investigating the force-velocity curve of MR damper behaviour are performed for a set of constant values of applied current, and in this case 0.25, 0.5, 1, 1.5 and 2 Ampere and a cyclic motion of 1.08 Hz were used. The second step is to obtain the hard points from the experimental data from step one as illustrated in Figure 7. The hysteresis loop of each force-velocity curve is divided into two regions namely positive acceleration (upper loop) and negative acceleration (lower loop). Then the third step is fitting both the upper loop and lower loop by the polynomial function expressed as:

$$F = \sum_{i=0}^{n} a_i v^i, \quad n = 6 \tag{1}$$

where F is the damper force, a_i is the experimental coefficient to be determined from the curve fitting and v is the damper velocity. In this work, the order of the polynomial for the damping force model is chosen by trial and error. After several investigations, it is observed that sixth order or higher order polynomials are able to capture the hysteresis behaviour of MR damper. Considering computational time and implementation in real-time control of the damper, a sixth order polynomial is selected. This method was also used by Du et al. (2005) and an 11th order polynomial has been selected to model the MR damper manufactured by Lord Corporation.

Figure 7 Hard points taken from the experimental result

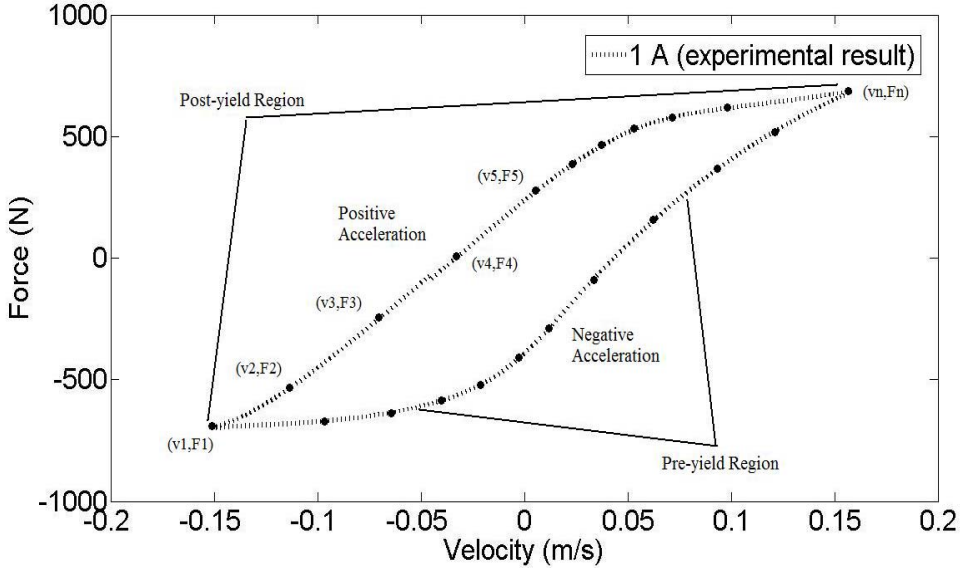

The fourth step is linearisation of the coefficient a_i for each curve. In this step, the coefficient of a_i is linearly approximated with respect to the input current (Choi et al., 2001; Du et al., 2005). The linearisation of the coefficient a_i is governed as follows:

$$a_i = b_i + I.c_i, \quad i = 0,1,2,\ldots,6 \tag{2}$$

After substituting equations (2) into (1), the damping force can be expressed as follows:

$$F = \sum_{i=0}^{n} \left(b_i + I.c_i\right) v^i, \quad n = 6 \tag{3}$$

The coefficients of b_i and c_i are obtained from the slope and the intercept of the plots as shown in Figure 8. From the investigation, the coefficients of a_i, b_i and c_i are not responsive to the magnitude of the applied current. The values of b_i and c_i used in this study are listed in Table 1.

In the last step, the output of the model namely damper force is selected by a switch block. The switch block will pass through the output of positive acceleration subsystem if the acceleration of the damper is greater or equal to zero. Otherwise, the switch block will pass through the output of negative acceleration subsystem.

Figure 8 The linear regression of the coefficients a_i correspond to the input current (see online version for colours)

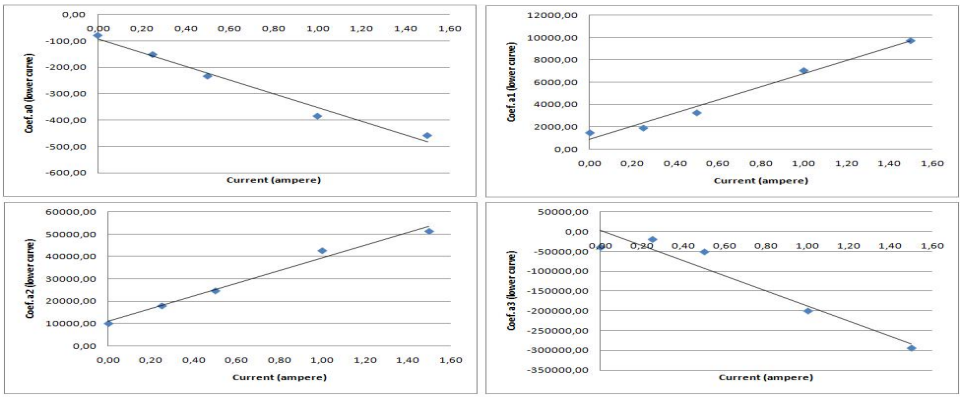

Table 1 Coefficients of the sixth order polynomial model

Negative acceleration			
Parameter	*Value*	*Parameter*	*Value*
b_0	–92,06270	c_0	–260,29500
b_1	864,87348	c_1	5876,28110
b_2	10847,50000	c_2	28450,00000
b_3	3373,79310	c_3	–191522,75860
b_4	–45927,06897	c_4	–1566475,86200
b_5	–676829,31030	c_5	4647275,86200
b_6	7033362,06900	c_6	34594827,59000
Positive acceleration			
Parameter	*Value*	*Parameter*	*Value*
b_0	82,9446	c_0	159,3602
b_1	1567,7540	c_1	4551,6440
b_2	–19780,9000	c_2	4957,1190
b_3	–69390,3000	c_3	–26713,4000
b_4	1257495,2590	c_4	–1242506,5520
b_5	1184779,3100	c_5	104524,1379
b_6	–24121551,7200	c_6	31239310,3400

4 Semi-active suspension control

4.1 Controller structure

The controller structure implemented in this study is shown in Figure 9, which consists of two loops namely outer and inner loops. The outer loop controller is used for disturbance rejection control that is to reduce unwanted vehicle's motions. The inputs of the outer

loop controller are vehicle states namely body velocity and wheel velocity, whereas the output of the outer loop controller is the desired damping force that must be tracked by the MR damper. The inner loop controller is used for force tracking control of the MR damper in such a way that the force produced by the MR damper is as close as possible with the desired force generated by the outer loop control.

A quarter car model is considered in this study. A quarter car model with a passive suspension system consists of one-fourth of the body mass, suspension components and one wheel as shown in Figure 10(a). A quarter car model with a semi-active suspension system where a MR damper is installed in parallel with the spring of passive suspension system is shown in Figure 10(b). The assumptions of a quarter car modelling are the tyre is modelled as a linear spring without damping, there is no rotational motion in wheel and body, the behaviour of spring and damper are linear, the tyre is always in contact with the road surface and effect of friction is neglected so that the residual structural damping is not considered in the vehicle model.

Figure 9 The controller structure of semi-active suspension system

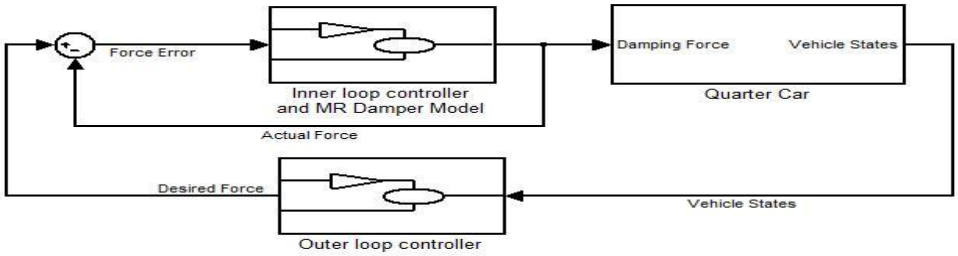

Figure 10 Passive and semi-active quarter car model

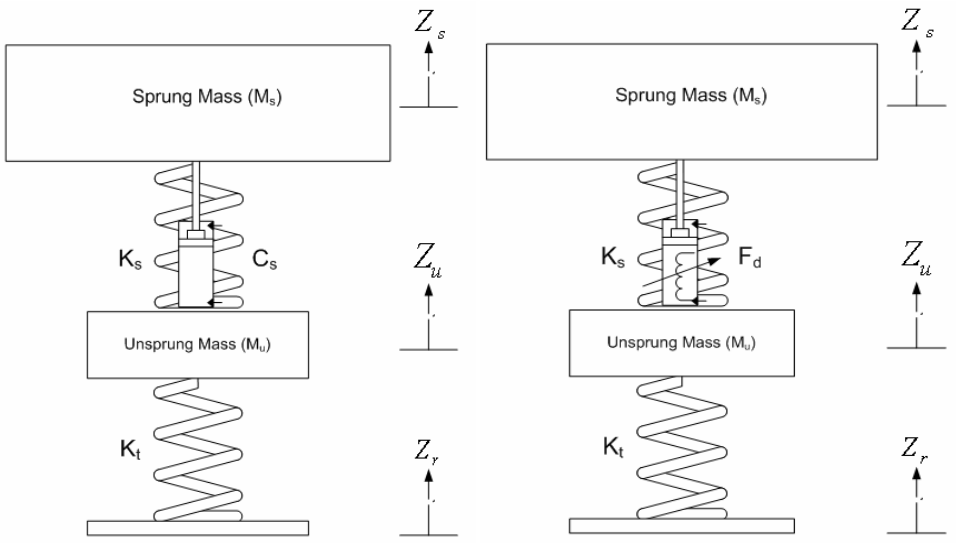

(a) (b)

The equations of motion of the passive suspension model which are shown in Figure 10(a) are given by:

$$M_s\ \ddot{z}_s + C_s\left(\dot{z}_s - \dot{z}_u\right) + K_s\left(z_s - z_u\right) = 0 \tag{4}$$

$$M_u\ \ddot{z}_u + C_s\left(\dot{z}_u - \dot{z}_s\right) + K_s\left(z_u - z_s\right) = 0 \tag{5}$$

The equations of motion of the semi-active suspension model shown in Figure 10(b) are given by:

$$M_s\ \ddot{z}_s - F_d + K_s\left(z_s - z_u\right) = 0 \tag{6}$$

$$M_u\ \ddot{z}_u + F_d + K_s\left(z_u - z_s\right) + K_t\left(z_u - z_r\right) = 0 \tag{7}$$

where

M_s sprung mass (kg)

M_u unsprung mass (kg)

z_r road profile (m)

z_s sprung mass displacement (m)

z_u unsprung mass displacement (m)

K_s spring stiffness (N/m)

C_s damping constant (N.s/m)

K_t tyre stiffness (N/m)

F_d semi-active damper force (N).

The performance criteria of the suspension system to be investigated are body acceleration, body displacement, suspension working space and wheel acceleration (Hudha et al., 2005).

4.2 Inner loop controller

The performance of the force-tracking control of the proposed MR damper model is presented based on simulation and experimental studies. The simulation study was executed in MATLAB-SIMULINK environment using sinusoidal, square and saw-tooth function of desired force. The structure of force tracking control of the proposed MR damper model using a simple PI control is shown in Figure 11. The PI controller is formulated as follows:

$$u(t) = K_p e(t) + K_i \int e(t)dt \tag{8}$$

$$e(t) = F_d(t) - F_a(t) \tag{9}$$

where F_d is the desired damping force and F_a is the actual damping force. In this simulation study, the parameters of K_p and K_i are chosen by trial and error method, where the values of K_p and K_i are set to 0.00769 and 0.000769 respectively.

Figure 11 The structure of force tracking control of MR damper

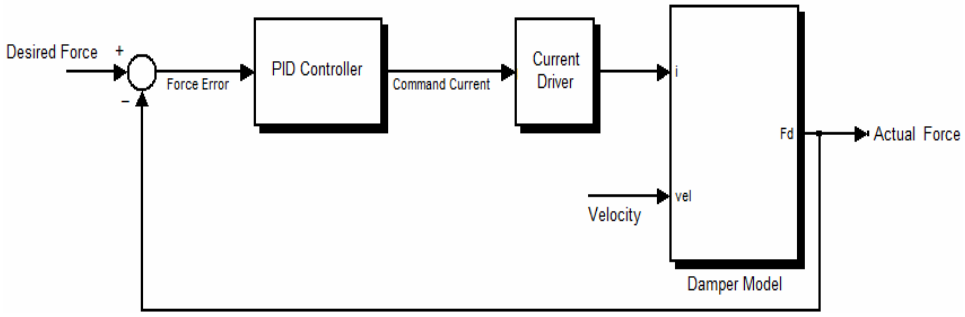

4.3 Outer loop controller

4.3.1 On-off skyhook control

Skyhook control strategy was introduced by Karnopp and Crosby (1973). As the name implies, the skyhook configuration shown in Figure 12 has a damper mounted on the vehicle body connected to some inertial reference in the sky. With the skyhook configuration, the trade-off between resonance control and high frequency isolation, common in passive suspension, is eliminated (Karnopp et al., 1974; Andersen, 2001). Notice that skyhook control focuses on the sprung mass; as C_{sky} increases, the sprung mass motion decreases. The skyhook configuration excels at isolating the sprung mass from base excitations, at the expense of increased unsprung mass motion.

Figure 12 Ideal skyhook damper configurations

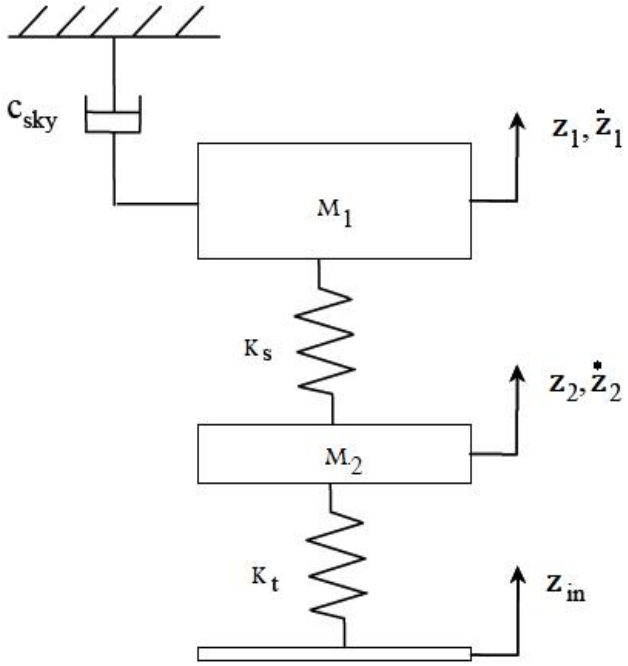

In essence, this skyhook configuration increases the damping coefficient to the sprung mass and reduces the damping coefficient from the unsprung mass. The skyhook configuration is ideal if the primary goal is isolating the sprung mass from base excitation, even at the expense of excessive unsprung mass motion (Karnopp *et al.*, 1974). Since this damper configuration is unrealisable in real automotive application, a controllable damper is often used to achieve a similar response to the system modelled in Figure 13. The semi-active damper is commanded such that it acts like a damper connected to an inertial reference in the sky. Figure 14 shows the semi-active equivalent model with the use of semi-active damper.

Figure 13 Equivalent model of ideal skyhook configuration

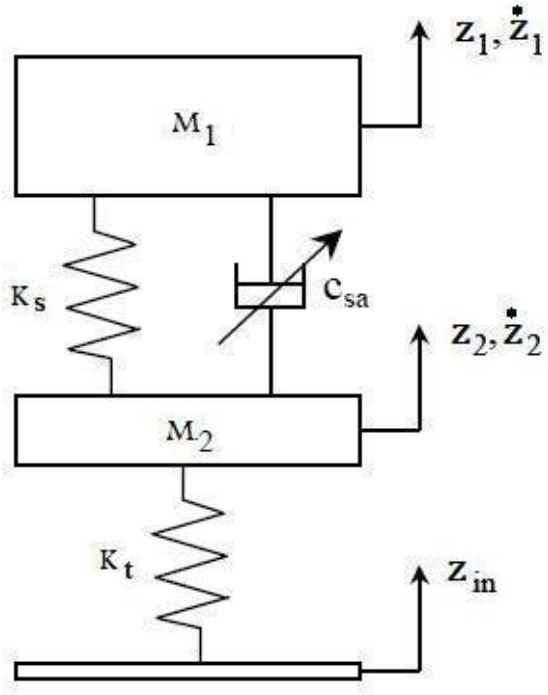

The simplest skyhook control is known as the on-off strategy which is referred to as high-state and low-state. The determination of whether the damper is to be adjusted to either its high-state or its low-state depends on the product of the relative velocity across the damper and the absolute velocity of the vehicle body mass attached to that damper. If the product is positive or zero, the damper is adjusted to its high-state; otherwise, the damper is set to low-state. This concept is summarized by:

$$F_d = C_{high}\left(\dot{z}_1 - \dot{z}_2\right) \quad \text{if} \quad \dot{z}_1\left(\dot{z}_1 - \dot{z}_2\right) > 0 \tag{10}$$

$$F_d = C_{los}\left(\dot{z}_1 - \dot{z}_2\right) \quad \text{if} \quad \dot{z}_1\left(\dot{z}_1 - \dot{z}_2\right) \le 0 \tag{11}$$

where F_d is the damping force; C_{high} and C_{low} are the high and low state damping constants respectively; $(\dot{z}_1 - \dot{z}_2)$ is the relative velocity between the sprung mass and unsprung mass and $\dot{z}_1$ is the absolute velocity of the unsprung mass. In this idea, the

value of the control signal is assumed to be switched from a hard to a soft damping coefficient.

4.3.2 Continuous skyhook control

In continuous skyhook control, there still exist a high-state and a low-state of damping as in the on-off damping control policy. However, it is not limited to these states alone. They may exist at any value within the two states. The damper force in the semi-active case must be equal to the damper force in the ideal skyhook case as given by (Motta et al., 2000):

$$F_s = C_s \dot{z}_1 \tag{12}$$

$$F_u = u\left(\dot{z}_1 - \dot{z}_2\right) \tag{13}$$

and

$$F_s = F_u \tag{14}$$

so that,

$$u = C_s \frac{z_1}{\left(z_1 - z_2\right)} \tag{15}$$

where F_s is the ideal skyhook damping force; F_u is the semi-active damper force; C_s is the skyhook damping coefficient and u is the semi-active damping coefficient.

The desired value of F_u is $C_s \dot{z}_1$, however, the semi-active device will only be able to generate this force depending on the sign of the product of the body velocity and the damper velocity. The only power required for the semi-active suspension is to activate the MR fluid to switch the value of the damping coefficient. Thus,

$$u = C_d \quad \text{if} \quad \dot{z}_1\left(\dot{z}_1 - \dot{z}_2\right) > 0 \tag{16}$$

$$u = C_{\min} \quad \text{if} \quad \dot{z}_1\left(\dot{z}_1 - \dot{z}_2\right) \le 0 \tag{17}$$

where $C_{\min}$ is the minimum damping coefficient of the continuous skyhook. Here, C_d is given by (Motta et al., 2000):

$$C_d = C_{\max} \quad \text{if} \quad C_s \frac{z_1}{\left(z_1 - z_2\right)} > C_{\max} \tag{18}$$

$$C_d = C_s \frac{z_1}{\left(z_1 - z_2\right)} \quad \text{if} \quad C_p < C_s \frac{z_1}{\left(z_1 - z_2\right)} \le C_{\max} \tag{19}$$

$$C_d = C_p \quad \text{if} \quad C_s \frac{z_1}{\left(z_1 - z_2\right)} \le C_p \tag{20}$$

where $C_{\max}$ is the maximum damping coefficient of the continuous skyhook control and C_p is the passive damping coefficient.

4.3.3 Skyhook algorithm-based fuzzy logic control

It should be noted that the conventional skyhook algorithm treats all conditions without considering the moving direction between sprung and unsprung masses. It is obvious that all cases should be treated differentially. Fuzzy logic is good to handle such a need because the desired damping constant can be determined by considering the moving direction between sprung and unsprung masses (Craft et al., 2003; Goncalves and Ahmadian, 2003). The output of the controller as determined by the fuzzy logic may exist anywhere between the high and low states damping.

In fuzzy logic development, it is important to define certain parameters and conventions that will be used throughout the controller development. Referring to the Figure 14, for all sign assignment, up is positive and down is negative. Several conditions will occur during vertical motion. The first case is when the sprung mass is moving upwards and the two masses are separating. The second is when the sprung mass moving downwards and the two masses are coming together. It follows with the sprung mass is moving upwards and the two masses are coming together. Finally, when the sprung mass is moving downwards and the two masses are separating. All of the cases will be considered in defining the appropriate damping constant.

Basically, a fuzzy logic controller consists of the fuzzification of the controller inputs, the execution of the rules of the controller and the defuzzification of the output to a crisp value to be implemented by the controller. The first step of a fuzzy logic controller is the fuzzification of the controller inputs in which it is accomplished through the structure of a membership function for each of the input. For the quarter car system, the fuzzy logic controller is designed with two inputs namely the sprung mass velocity $\dot{z}_1$ and the relative velocity across the damper $\dot{z}_{12}$. The possible shapes of these membership functions are infinite, though the shapes that are most widely used are the triangular-type, trapezoidal-type, Gaussian-type, and singleton membership functions (Carter, 1998). In this study, a Gaussian-type is used for each input. Each membership function is defined by three linguistic variables, Negative (N), Zero (Z) and Positive (P), and is symmetric about zero. Figure 14(a) and 14(b) define each input and their membership functions.

Figure 14 Input membership function, (a) absolute sprung mass velocity $\dot{z}_1$ (b) relative velocity across the damper

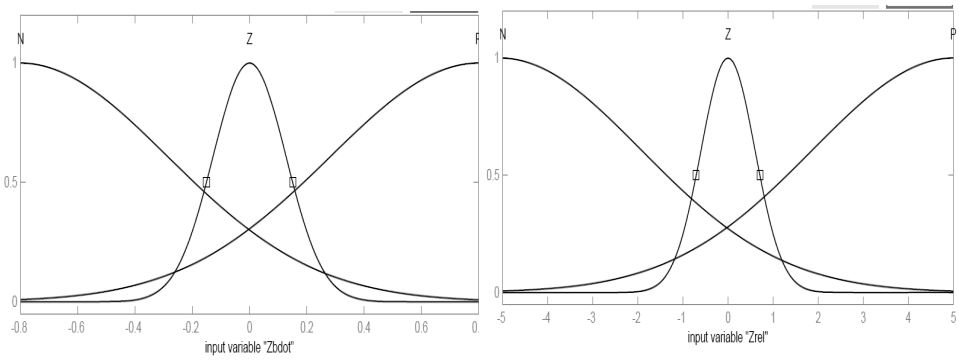

(a) (b)

The second step is the execution of the rule of the controller, in which the generic form of the fuzzy rule is as follows:

If $\dot{z}_1$ is (A) and $\dot{z}_{12}$ is (B) then C_d is (C)

where A, B and C represent the linguistic values for the absolute sprung mass velocity, the relative velocity across the damper and the desired damping coefficient respectively. In this study, fuzzy type used is Sugeno type and therefore the prescribed output values are constant. The prescribed output values of the fuzzy systems are listed in Table 2, in which the values are determined by choosing several damping constant values between the high and low states damping. Each is described by six linguistic variables as follows:

$$L = \left(C_p, C_{d1}, C_{d2}, C_{d3}, C_{d4}, C_{\max}\right) \tag{21}$$

The rules of the system can now be developed. The fuzzy logic controller rule-base for the quarter car model is detailed in Table 3.

Table 2 Prescribed output values of fuzzy system

L	*Value*
C_p	700
C_{d1}	3,000
C_{d2}	6,000
C_{d3}	9,000
C_{d4}	12,000
C_{max}	15,000

Table 3 Fuzzy logic rule

		$\dot{z}_{12}$		
		N	Z	P
$\dot{z}_1$	N	$C_{\max}$	C_{d1}	$C_{\min}$
	Z	C_{d4}	C_{d2}	C_{d3}
	P	$C_{\min}$	C_{d3}	$C_{\max}$

The fuzzy logic rule shown in Table 3 may be referred by skyhook-based fuzzy logic control. By examining the rule table, it can be seen that the rule is in agreement with the skyhook policy since both the absolute sprung mass velocity and the relative velocity across the damper are fully negative or fully positive. The $C_{\max}$ is defined as the maximum damping coefficient and will be employed since two input variables have the positive or negative sign which is known to be fully positive. When the product between each input variables has a negative sign, it can be called as fully negative in which the $C_{\min}$ is employed. However, when each input is not fully positive or fully negative, the fuzzy skyhook is used according to the membership function.

The last step is defuzzification which converts the fuzzy values obtained from execution of the rule tables into a single crisp value. The non-linear behaviour of the

fuzzy system can be recognized from the 3D graphical representation as shown in Figure 15. The output of the outer-loop controller is the desired damping coefficient C_d. However, the inner loop controller needs desired damping force F_d. as the controller input. Thus, the desired damping force can be obtained by multiplying the desired damping coefficient with the damper velocity $\dot{z}_p$ as follows:

$$F_d = C_d \dot{z}_p \tag{22}$$

Figure 15 Surface map of proposed fuzzy system

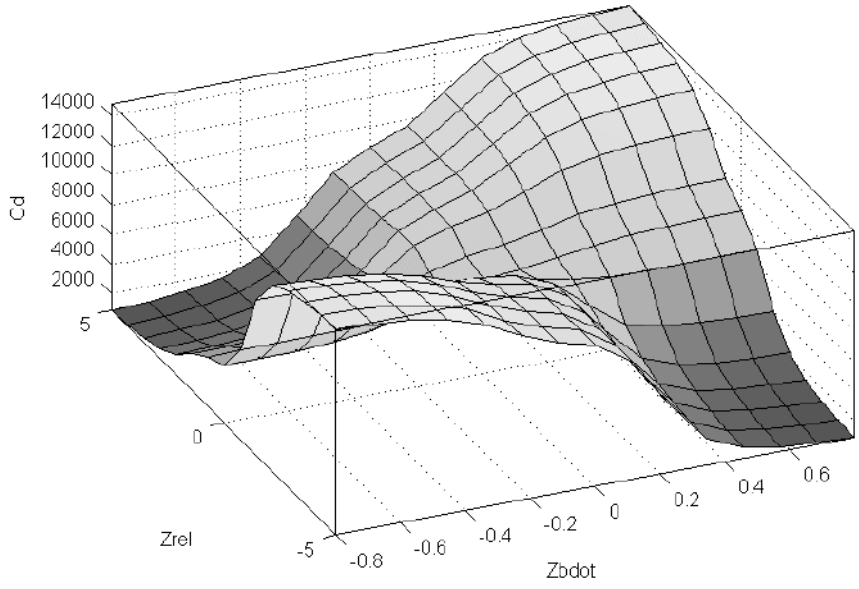

5 Simulation results

5.1 Validation of the MR damper model

Simulation was performed to explore the validity and the accuracy of the proposed model in Matlab-Simulink environment. The parameters of the inverse model were created based on minimising the error between the forces predicted by the model (F_d) with the actual force (F_a) obtained experimentally. The objective function, J is given as:

$$J = \sum_{i=1}^{n} \left(F_{ai} - F_{di} \right)^2 \tag{23}$$

where n is the total number of experimental data values in one cycle of excitation.

The hard points of the proposed model were obtained from the experimental data. The response of the proposed model is compared with the experimental data of force-velocity characteristics. During the simulation study, the excitation frequency and magnitude chosen were 1.08 Hz and ± 0.021 m respectively. These parameters are based on the experimental work. The overall comparison of force-velocity and force-displacement

characteristics under various input currents between experimental data and polynomial model responses are shown in Figures 16 and 17 respectively. From these figures, it can be seen that the proposed polynomial model is able to closely follow the experimental data in both post-yield and pre-yield regions.

Figure 16 Force-velocity characteristics comparison

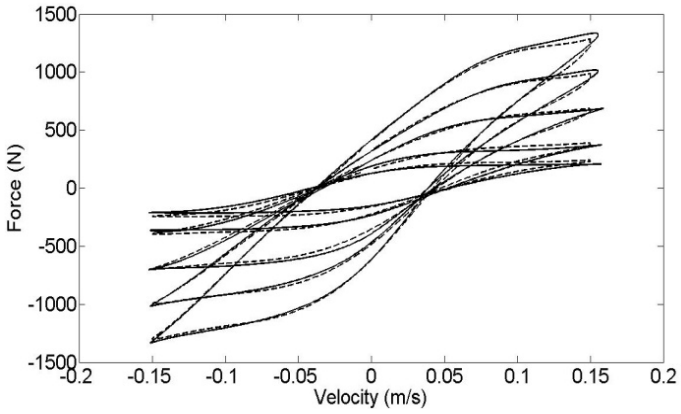

Note: Solid line indicates experimental result and dashed line indicates simulation results.

Figure 17 Force-displacement characteristics comparison

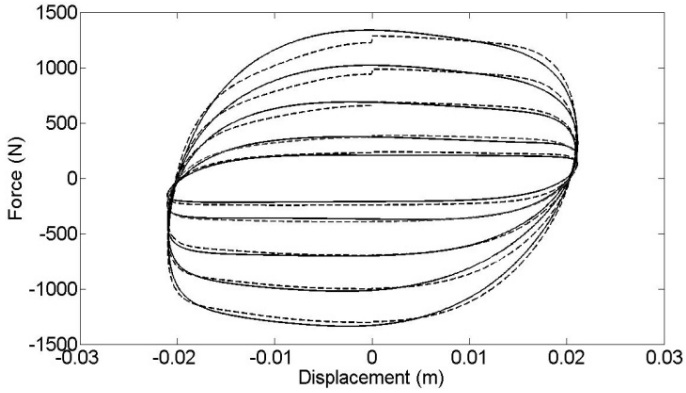

Note: Solid line indicates experimental result and dashed line indicates simulation results.

5.2 Force tracking control

The simulation results in response to various functions of desired force are shown in Figure 19. Force tracking control is intended to check the tracking ability for a class of continuous and discontinuous functions. From the simulation study, it can be seen clearly that the simulation results show the tracking ability of the damping force is realised by the close-loop controller. From Figure 18, it can be concluded that the sixth order polynomial model of MR damper has a good capability in tracking the desired force in the whole range of the piston velocity.

Figure 18 Force tracking control of desired force, (a) sinusoidal function (b) square function (c) saw-tooth function

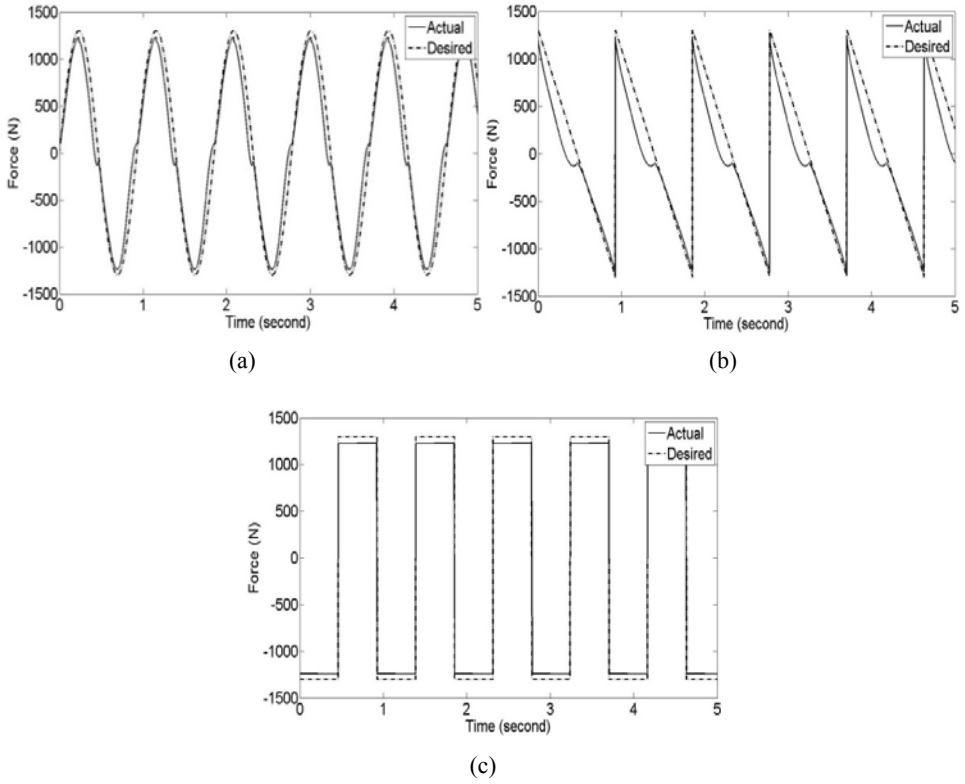

5.3 Time domain simulation

The simulation was performed for a period of 10 seconds using Bogacki-Shampine solver with a fix step size of 0.01 second. The type of road disturbance considered in this study is sinusoidal function with the amplitude of 0.021 m. It is important to establish the accuracy of the quarter car model by comparing computer simulation results with experimental data collected from an instrumented quarter car test rig equipped with a passive shock absorber. The numerical values of the quarter car model parameters are as follows:

M_s 170 kg

M_u 35 kg

K_s 16,000 N/m

K_t 200,000 N/m

C_s 700 Ns/m.

Figures 20(a) and 20(b) show the model validation results of the sprung mass acceleration for 0.8 and 1.1 Hz respectively. The comparison between simulation and experimental results displays good agreement with small difference in terms of

amplitude. The small error between the two data may occur due to the additional structural vibration recorded by the accelerometer including the friction between sliding bush and sliding shaft surface.

Figure 19 Model validation for sprung mass acceleration response, (a) 0.8 Hz (b) 1.1 Hz

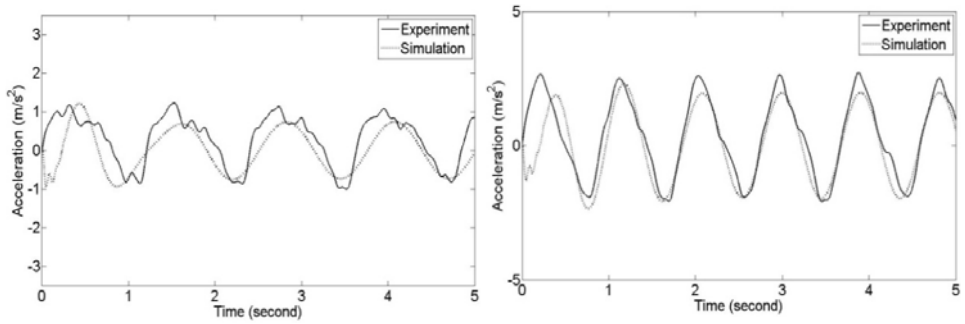

(a) (b)

The validation results between simulation and experimental work of sprung mass displacement response are displayed in Figures 20(a) and 20(b) for 0.8 and 1.1 Hz respectively. Similar observations as the sprung mass acceleration validation results, a small difference between the simulation and experimental results are observed. The sprung mass displacement responses are obtained by taking double integral of the sprung mass acceleration data. It is well known that an integration process is sensitive since it is influenced by the steady state error resulting from noise. This will also affect the sprung mass displacement trend and amplitude.

Figure 20 Model validation for sprung mass displacement response, (a) 0.8 Hz (b) 1.1 Hz

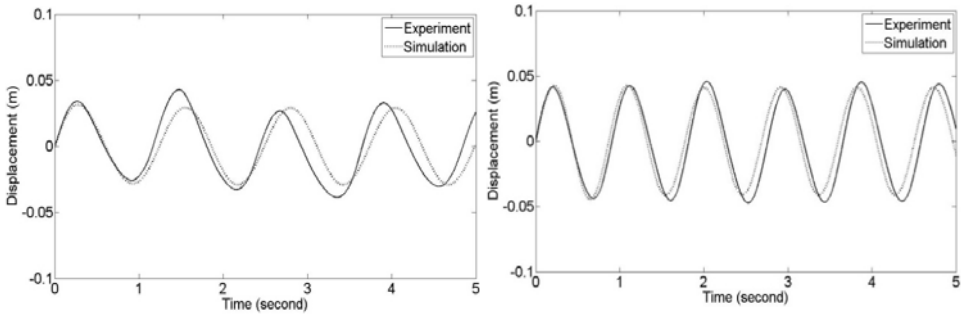

(a) (b)

In the experimental work, an LVDT was mounted between sprung mass and unsprung mass to measure the suspension travel. The dynamic responses of the suspension travel are shown in Figures 21(a) and 21(b) for 0.8 and 1.1 Hz excitation frequencies respectively. It can also be obtained by subtracting the double integral result of both sprung mass and unsprung mass accelerations. However, it is not recommended to use secondary data since the implementation of sensor is possible in real application. From

Figures 21(a) and 21(b), it can be seen that small difference occurs in terms of amplitude and trend. However, the simulation results are acceptable since it is relatively close to the experimental results.

Figure 21 Model validation for suspension travel response, (a) 0.8 Hz (b) 1.1 Hz

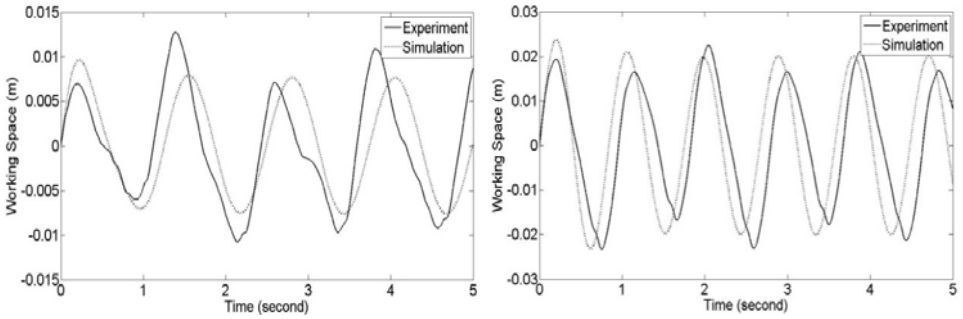

(a) (b)

Figures 22(a) and 22(b) show the unsprung mass acceleration response. In this system, the tyre is represented by an air spring which the springing characteristic of pressurised air is affected by the non-linear compressibility of the air. Whereas, during simulation study, the tyre is modelled by a linear spring which has a linear characteristic in term of force versus displacement. From Figure 22, it can be seen that the trend of the experimental results are not smooth as compared with the sinusoidal wave resulted from the simulation results. This may be caused by the non-linearity of the tyre as mentioned before. However, the results are still acceptable since the differences in term of trend and amplitude are very small.

Figure 22 Model validation for unsprung mass acceleration response, (a) 0.8 Hz (b) 1.1 Hz

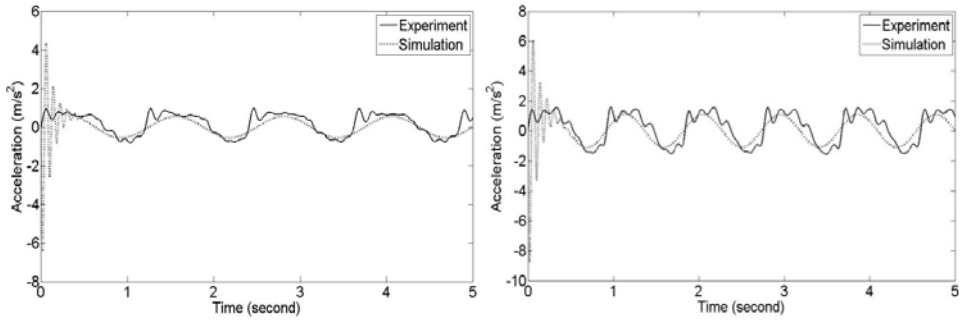

(a) (b)

The performance of the semi-active controllers in generating the desired variable damping constant is also investigated by applying sinusoidal road input with the frequency of 1.3, 8 and 17 Hz. The excitation frequencies chosen correspond to the frequencies below body natural frequency, between body and wheel natural frequency and above wheel natural frequency respectively, in which the natural frequency of the validated model both sprung and wheel is 1.57 Hz and 12.35 Hz respectively. The

controller parameters of 'on-off' skyhook and continuous skyhook are summarised in Table 4. While, the parameters of skyhook-based fuzzy logic control have been described in Section 4.3.3. It is noted that the selection of the damping constants used in the controller parameters is based on the ability of the damper in generating equivalent damping constants.

Table 4 The parameter of the skyhook controller

Criteria	*On-off skyhook (Ns/m)*	*Continuous skyhook (Ns/m)*
C_{high}	15,000	-
C_{low}	700	-
C_{min}	-	700
C_p	-	700
C_s	-	5,000
C_{max}	-	15,000

The results of ride performance in terms of sprung mass displacement, sprung mass acceleration, suspension travel and unsprung mass acceleration are presented in root-mean-square (RMS) value as listed in the Tables 5, 6, 7 and 8. Tables 5 and 6 list the RMS values of the sprung mass acceleration and displacement. From the tables, it can be seen that the semi-active suspension system using on-off skyhook, continuous skyhook and fuzzy logic control-based skyhook algorithm show significant improvement compared to the passive suspension system. Unwanted vibratory motions of vehicle body can be suppressed significantly by the semi-active suspension system resulting in improved ride performance. The simulation results shows fuzzy logic control is superior compared with its counterparts.

Tables 7 and 8 summarise the RMS values of the suspension travel and unsprung mass acceleration responses of the semi-active suspension system compared to the passive suspension system. It can be seen that there is no improvement in both suspension travel and wheel acceleration performances. The performance of suspension travel in semi-active system below the body natural frequency became worse than the passive system. However, the amount of the performance degradation decreases due to the increase of the excitation frequency. This shortcoming is still acceptable since the suspension travel at low frequency vibration can be ignored. This is due to the fact that the fatigue life of the damper dominantly depends on the magnitude of the suspension travel at medium and high frequency vibration (Li et al., 2000). It can be concluded that the semi-active suspension system is effective in damping out the motions of vehicle body with the consequence of impairing suspension displacement and wheel acceleration.

Table 5 RMS values for sprung mass acceleration

Frequency	*Passive*	*On-off*	*%*	*Continuous*	*%*	*Fuzzy*	*%*
1.3 Hz	2.5020	1.9698	21.27	1.7966	28.19	1.5732	37.12
8 Hz	5.6750	3.81886	32.71	3.6137	36.32	3.2823	42.16
17 Hz	6.7172	4.6698	30.48	4.4208	34.19	3.9036	41.89

Table 6 RMS values for sprung mass displacement

Frequency	*Passive*	*On-off*	*%*	*Continuous*	*%*	*Fuzzy*	*%*
1.3 Hz	0.0369	0.02918	20.92	0.02661	27.89	0.0235	36.31
8 Hz	0.0023	0.00153	33.48	0.00145	36.96	0.0013	43.48
17 Hz	0.000688	0.000465	32.37	0.000443	35.57	0.00039	42.99

Table 7 RMS values for suspension travel

Frequency	*Passive*	*On-off*	*%*	*Continuous*	*%*	*Fuzzy*	*%*
1.3 Hz	0.0149	0.0172	–15.44	0.0179	–16.76	0.0183	–18.58
8 Hz	0.0236	0.0249	–5.51	0.0253	–6.72	0.0256	–7.81
17 Hz	0.0150	0.0155	–3.33	0.0158	–5.06	0.0159	–5.66

Table 8 RMS values for unsprung mass acceleration

Frequency	*Passive*	*On-off*	*%*	*Continuous*	*%*	*Fuzzy*	*%*
1.3 Hz	1.4204	1.57907	–11.17	1.7023	–19.85	1.7459	–22.92
8 Hz	58.0393	63.1226	–8.76	66.5931	–14.74	68.7207	–18.40
17 Hz	168.5647	180.187	–6.89	187.1368	–11.02	194.1556	–15.18

6 Experimental work

6.1 Experimental result of force tracking control

Although the simulation studies was conducted using a validated MR damper model, it is important to conduct the experimental work on force tracking control of MR damper. In this study, the experimental work was conducted using suspension test machine available at Autotronic Laboratory, UTeM using sinusoidal input at the frequency of 1.08 Hz and the excitation amplitude of 0.021 m. The experimental results of force tracking control were shown in Figure 23.

In the experimental work, it is important to note that the output voltage from the IMC device is in the form of pulse signal. The value of voltage applied to the current driver is represented by the width of the generated pulse. The higher the current applied to the MR damper by the current driver, the wider the voltage pulse width generated by the controller hardware to the current driver. From Figure 23, it can be seen that there is chattering effect at the peak value of the actual damping force especially for the desired forces of 500 N. The chattering effect may be due to the width of the pulse applied to the current driver in which the lower amplitude of the desired force, the tighter width of the pulse supplied. At the higher desired forces of 800 N, 1,100 N and 1,300 N, the chattering effect reduces significantly. However, it is still acceptable since the actual damping force tracked the desired damping force. From overall experimental results, it can be concluded that the PI control can realise the tracking ability of the damping force under various frequencies and desired forces, by allowing the chattering effect appears at the lower region of damping force.

Figure 23 The experimental results of force tracking control under several sinusoidal amplitudes of the desired forces at the frequency of 1.08 Hz, (a) 500 N (b) 800 N (d) 1,100 N (d) 1,300 N

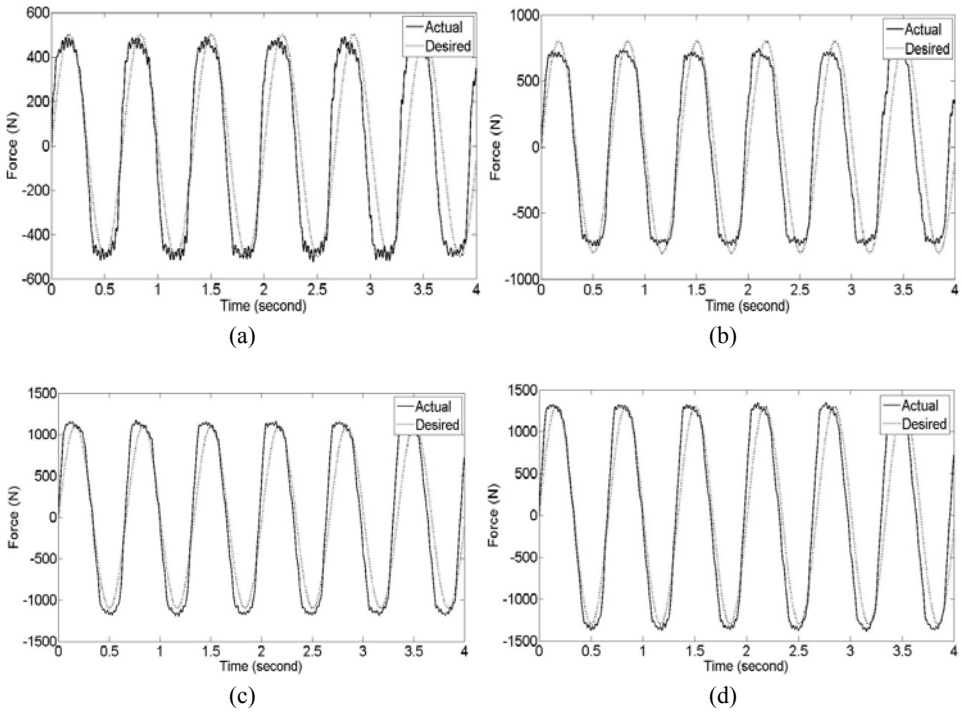

6.2 Performance evaluation on a quarter car test rig

To verify and validate the control system proposed, an experimental work using the quarter car test rig has been conducted. The implementation of conventional skyhook and fuzzy logic control were evaluated for its performance at controlling the sprung and unsprung masses according to sprung mass acceleration, sprung mass displacement, suspension travel and unsprung mass acceleration (Hudha et al., 2005). Figures 24 to 27 show the experimental results of passive and semi-active suspension system. The controller parameters of the proposed controller are set the same with the controller parameters obtained from the simulation study.

Figures 24(a), 24(b) and 24(c) shows significant improvements on the sprung mass acceleration of semi-active suspension system with fuzzy logic control over its counterparts. It is observed that the RMS values of body acceleration for semi-active suspension using on-off skyhook at the excitation frequencies of 0.8 Hz, 1.1 Hz and 1.3 Hz are 0.5723 m/s^2, 1.296 m/s^2 and 2.7088 m/s^2 respectively. While for the semi-active suspension using continuous skyhook are 0.5475 m/s^2, 1.2363 m/s^2 and 2.4611 m/s^2 respective to the excitation frequencies. The superiority of semi-active suspension using fuzzy logic control is shown by the RMS values of 0.5132 m/s^2, 1.1702 m/s^2 and 1.9588 m/s^2 which are less than its counterparts. Table 9 summarises the RMS values of the sprung mass acceleration responses. From the table, it can be seen that overall the performance of the semi-active suspension system is better than the passive

system. However, fuzzy logic control gives user better results in terms of reduction percentage. The improvements achieved by fuzzy logic control are 24.08%, 22.29% and 27.67%.

Figure 24 Sprung mass acceleration responses, (a) 0.8 Hz (b) 1.1 Hz (c) 1.3 Hz

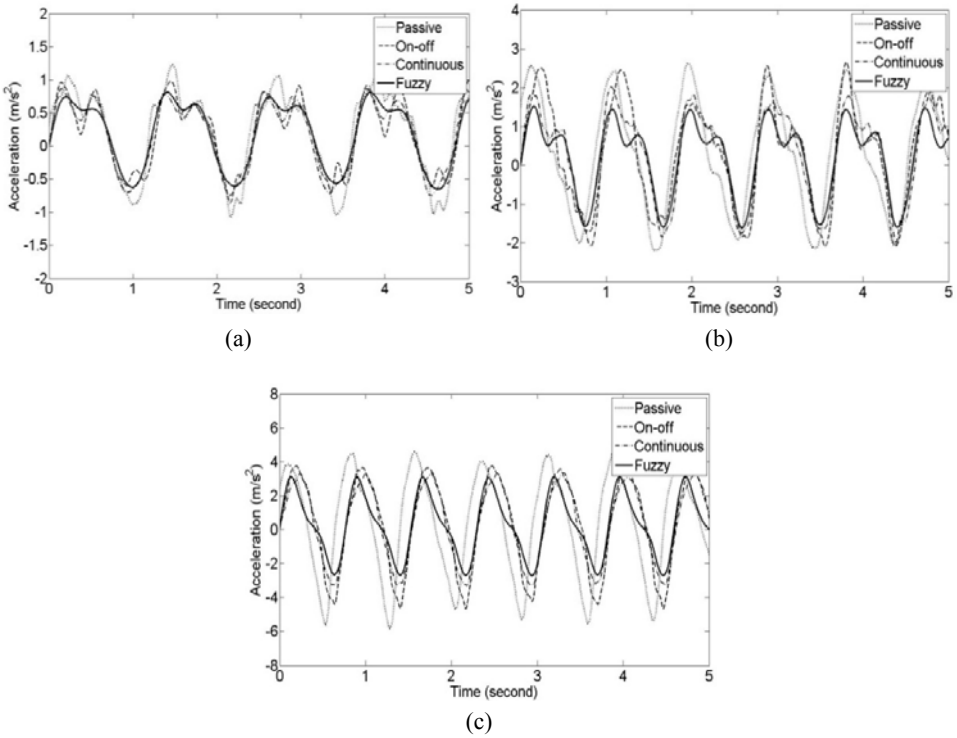

Table 9 RMS values of the sprung mass acceleration

Frequency	*Passive*	*On-off*	*%*	*Continuous*	*%*	*Fuzzy*	*%*
0.8 Hz	0.676	0.5723	15.34	0.5475	19.01	0.5132	24.08
1.1 Hz	1.506	1.296	13.94	1.2363	17.91	1.1702	22.29
1.3 Hz	3.091	2.7088	12.36	2.4611	20.38	1.9588	27.68

The semi-active suspension system using fuzzy logic control also offers significant improvement on sprung mass displacement as shown in Figures 25(a), 25(b) and 25(c). Figure 25 describes the sprung mass displacement for semi-active and passive suspension system, in which the sprung mass displacement responses of semi-active suspensions with all controllers implementation show the superiority over the passive suspension system. The RMS values of sprung mass displacement for semi-active system with on-off skyhook for 0.8 Hz, 1.1 Hz and 1.3 Hz are 0.0184 m, 0.0259 m and 0.04 m, while using continuous skyhook are 0.0176 m, 0.0249 m and 0.0344 m respectively. Using fuzzy logic control, the RMS values are lower than that of using both on-off and continuous skyhook, in which its values are 0.0166 m, 0.0235 m and 0.0323 m.

Table 10 lists the RMS values of the sprung mass displacement responses. The reduction percentages achieved by implementing on-off skyhook control are 16.05%, 15.35% and 8.88%. While using continuous skyhook control, the improvements achieved are 19.65%, 18.62% and 21.64% which is higher than passive system and semi-active system using on-off skyhook. The best performance in decreasing sprung mass displacement is achieved by fuzzy logic control which has the reduction percentages of 25.54%, 23.20% and 26.42%. The whole experimental results proof that semi-active MR damper using direct fuzzy logic control can suppress body vibration better than that of implementing skyhook control. It can also be concluded that the semi-active system could provide significant improvement on ride performance.

Figure 25 Sprung mass displacement responses, (a) 0.8 Hz (b) 1.1 Hz (c) 1.3 Hz

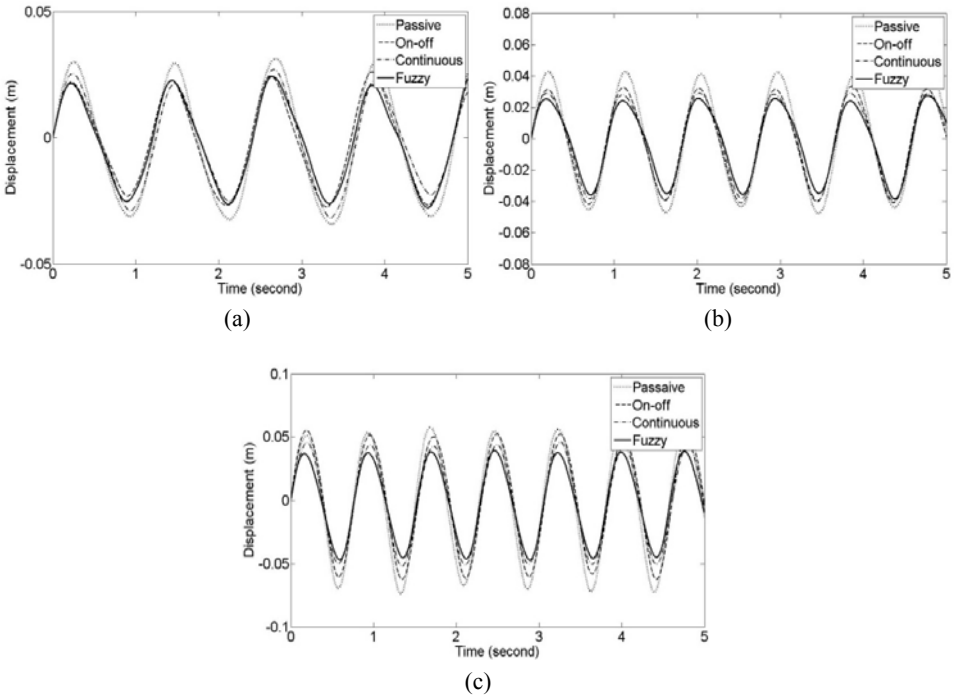

Table 10 RMS values of the sprung mass displacement

Frequency	*Passive*	*On-off*	*%*	*Continuous*	*%*	*Fuzzy*	*%*
0.8 Hz	0.022	0.0184	16.05	0.017632	19.85	0.0166	24.54
1.1 Hz	0.0306	0.0259	15.35	0.0249	18.62	0.0235	23.20
1.3 Hz	0.0439	0.04	8.88	0.0344	21.64	0.0323	26.42

Suspension travel responses of semi-active suspension system and passive suspension system are shown in Figures 26(a), 26(b) and 26(c) for the excitation frequencies of 0.8 Hz, 1.1 Hz and 1.3 Hz respectively. From the figures, it is clearly seen that semi-active suspension system shows worse performance over passive suspension system. The RMS values of the semi-active suspension system with on-off skyhook are

0.0063 m, 0.0141 m and 0.0238 m. Using continuous skyhook control, the overall values at each frequency are lower than using the on-off scheme. Table 11 summarises the RMS values of suspension travel response. Compared with skyhook control, fuzzy logic control has the lowest value of suspension travel performance decrement, in which the values are 7.41%, 3.79% and 2.18% respectively. Generally, it can be concluded that there is agreement between experimental and simulation results, in which the suspension travel responses of semi-active suspension system is also worse than the passive suspension system in below body natural frequency.

Figure 26 Suspension travel responses, (a) 0.8 Hz (b) 1.1 Hz (c) 1.3 Hz

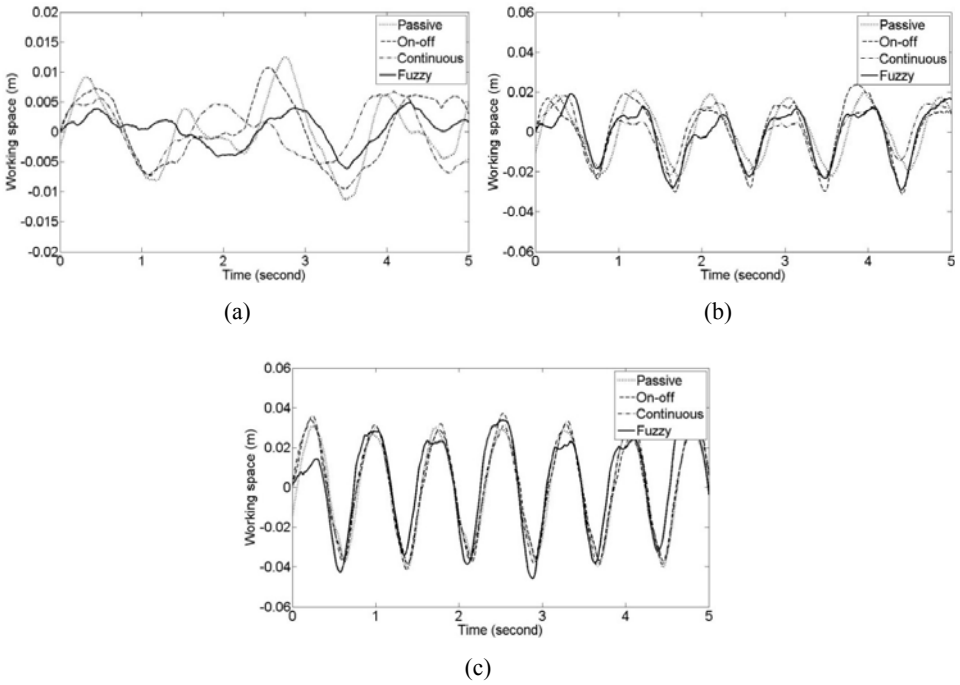

Table 11 RMS values of suspension travel

Frequency	*Passive*	*On-off*	*%*	*Continuous*	*%*	*Fuzzy*	*%*
0.7 Hz	0.0054	0.0063	–16.67	0.0061	–12.96	0.0058	–7.41
1.08 Hz	0.0132	0.0141	–6.82	0.0128	3.03	0.0137	–3.79
1.3 Hz	0.0229	0.0238	–3.93	0.0236	–3.06	0.0234	–2.18

The last performance criterion observed is unsprung mass acceleration response which is shown in Figures 27(a), 27(b) and 27(c). It is noted that there is no improvement on unsprung mass acceleration by implementing semi-active suspension system. The RMS values of unsprung mass acceleration response of the passive suspension system for 0.8 Hz, 1.1 Hz and 1.3 Hz are 0.5816 m/s^2, 1.0685 m/s^2 and 2.1225 m/s^2. While the RMS values of semi-active suspension system with on-off skyhook are 0.6307 m/s^2,

1.1768 m/s^2 and 2.3867 m/s^2. Using continuous skyhook, the RMS values are 0.651 m/s^2, 1.1502 m/s^2 and 2.5285 m/s^2. On the other hand, the RMS values by implementing fuzzy logic control are 0.6692 m/s^2, 1.1768 m/s^2 and 2.4833 m/s^2.

Table 12 helps to easy understand the performance of unsprung mass responses between semi-active and passive suspension systems. From the table, it can be seen that the implementation of several control algorithms deteriorates the unsprung mass performance. Implementing on-off skyhook control makes the unsprung mass response decreases about 8.44%, 10.14% and 12.45% for the excitation frequency of 0.8 Hz, 1.1 Hz and 1.3 Hz respectively. While using continuous skyhook control, the degradation reaches 11.93%, 7.65% and 19.13% which is higher than the semi-active response using on-off skyhook control. However, the worst RMS values occur in the implementation of fuzzy logic control. The decrement percentages are about 15.06%, 10.14% and 17%. There is an agreement between experimental and simulation results in which the proposed control system can only attenuate vehicle vibration by allowing excessive magnitude of wheel acceleration.

Figure 27 Unsprung mass acceleration responses, (a) 0.8 Hz (b) 1.1 Hz (c) 1.3 Hz

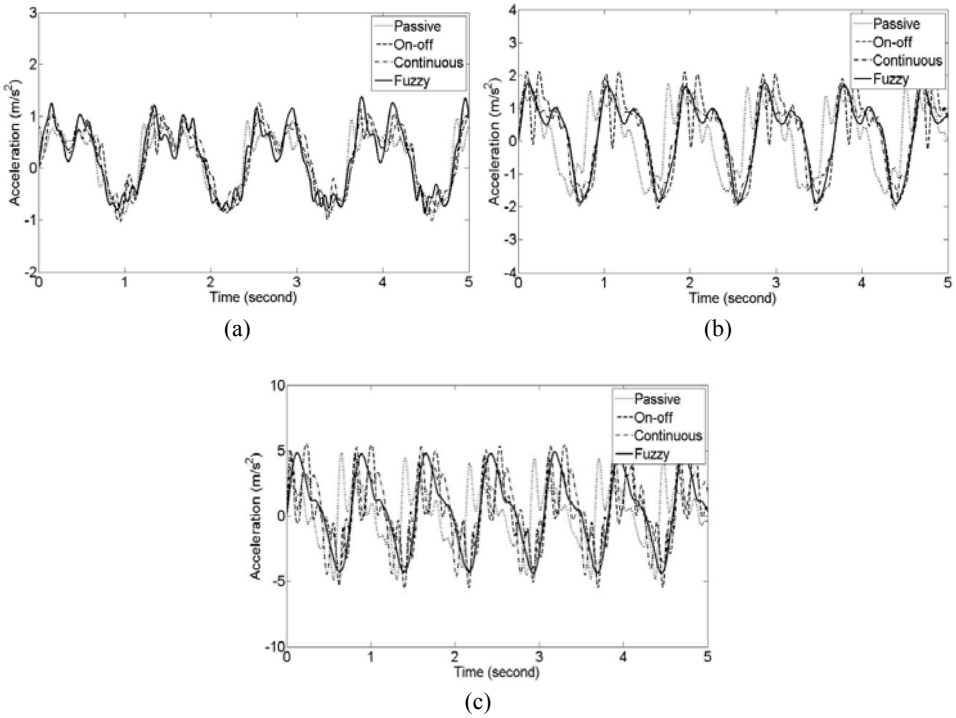

Table 12 RMS values of the unsprung mass acceleration

Frequency	*Passive*	*On-off*	*%*	*Continuous*	*%*	*Fuzzy*	*%*
0.8 Hz	0.5816	0.6307	–8.44	0.651	–11.93	0.6692	–15.06
1.1	1.0685	1.1768	–10.14	1.1502	–7.65	1.1768	–10.14
1.3	2.1225	2.3867	–12.45	2.5285	–19.13	2.4833	–17.00

7 Conclusions

One of the important factors to successfully achieve desirable control performance is having a damping force model which can accurately capture the non-linear hysteresis behaviour of MR damper. The proposed sixth order polynomial model for field-dependent damping force of MR damper has been investigated in this study. The measured experimental damping force was compared with the predicted ones from the proposed model. It has been demonstrated that the proposed model agrees well with the non-linear hysteresis behaviour of the MR damper in the form of force-velocity and force-displacement characteristics.

The tracking ability of the proposed model has been investigated in both simulation and experimental works by realising a simple closed-loop PI control. From simulation study, it can be seen clearly that under several input functions, the proposed polynomial model tracks the desired damping force well. To check the performance of the PI control, an experimental work has been performed under various frequencies and desired damping forces. It can be concluded that the PI control shows a good performance in tracking the desired damping force under various conditions.

In this study, vibration control characteristics of a semi-active quarter car system have been evaluated via both computer simulation and experimental work through an instrumented quarter car test rig. Three previously developed methods of semi-active damping control, referred to as on-off skyhook, continuous skyhook and skyhook-based fuzzy logic control. With on-off and continuous skyhook control, the sprung mass displacement and acceleration were significantly minimised, but at the expense of increased suspension travel and unsprung mass acceleration. The fuzzy logic control was tuned by adopting skyhook algorithm as its rules. Then, it was compared with the on-off and continuous skyhook semi-active control policies. The comparison results show that when tuned appropriately, the fuzzy logic controller is capable in improving most of the on-off and continuous skyhook response value.

References

Ahmadian, M. and Goncalves, F.D. (2004) 'A frequency analysis of semi-active control methods for vehicle application', *SAE Automotive Dynamics, Stability and Control Conference*, 4–6 May, Detroit, p.386.

Andersen, E.R. (2001) 'Multibody dynamics modeling and system identification for a quarter-car test rig with McPherson strut suspension', Master theses, Virginia Polytechnic Institute.

Buckner, G.D., Schuetze, K.T. and Beno, J.H. (2000) 'Active vehicle suspension control using intelligent feedback linearization', *Proc. of American Control Conference*, Chicago, pp.4014–4018.

Carlson, D.J. (2001) 'What makes a good MR fluid?', *International Conference on Electrorheological (ER) Fluids and Magnetorheological (MR) Suspensions*, 9–13 July, Nice.

Carter, A.K. (1998) 'Transient motion control of passive and semi-active damping for vehicle suspensions', Master theses, Virginia Polytechnic Institute.

Choi, S.B., Lee, S.K. and Park, Y.P. (2001) 'A hysteresis model for the field-dependent damping force of a magneto-rheological damper', *Journal of Sound and Vibration*, Vol. 245, No. 2, pp.375–383.

Craft, M.J., Buckner, G.D. and Anderson, R.D. (2003) 'Semi-active vehicle shock absorbers: design and experimental evaluations, *Proceedings of SPIE – The International Society for Optical Engineering*, SPIE, 3–6 March, San Diego, CA, pp.577–588.

Du, H., Yim, S.K. and Lam, J. (2005) 'Semi-active H_∞ control of vehicle suspension with magnetorheological dampers', *Journal of Sound and Vibration*, Vol. 283, No. 3, pp.981–996.

Gillespie, T.D. (1992) *Fundamentals of Vehicle Dynamics*, Society of Automotive Engineers, Warrendale, PA.

Goncalves, F.D. and Ahmadian, M. (2003) 'A hybrid control policy for semiactive vehicle suspensions', *Journal of Shock and Vibration*, Vol. 10, No. 1, pp.59–69.

Hennecke, D. and Zieglmeier, F.J. (1988) 'Frequency dependent variable suspension hamping – theoretical background and practical success', *Proceeding of Institution of Mechanical Engineers*, pp.101–111.

Hudha, K., Jamaluddin, H., Samin, P.M. and Rahman, R.A. (2005) 'Effect of control techniques and damper constrain on the performance of semi-active magnetorheological damper', *International Journal of Vehicle Autonomous System (IJVAS)*, Vol. 3, Nos. 2/3/4, pp.230–252.

Hudha, K., Jamaluddin, H., Samin, P.M. and Rahman, R.A. (2008) 'Non-parametric linearized data driven modeling and force tracking control of a magnetorheological damper', *International. Journal of Vehicle Design (IJVD)*, Vol. 46, No. 2, pp.250–269.

Hutton, R. (2001) 'Trio Appassionato: Ferrari FX, Lamborghini Murcielago, and Maserati Spyder', *Car and Driver Magazine*, December.

IMC (2002) *IMC-FAMOS User's Manual*, IMC GmbH., Berlin, Germany.

Jolly, M.R., Jonathan, W.B. and Carlson, J.D. (1998) 'Properties and applications of commercial magnetorheological fluids', *SPIE 5th Annual Int. Symposium on Smart Structures and Materials*, San Diego, CA, 15 March.

Karnopp, D.C. and Crosby, M.J. (1973) 'System for controlling the transmission of energy between spaced members', United States Patent #3,807,678.

Karnopp, D.C., Crosby, M.J. and Harwood, R.A. (1974) 'Vibration control using semi-active force generators', *Journal of Engineering for Industry*, Vol. 96, No. 2, pp.618–626.

Kazuoka, K. (1992) 'Development of high performance shock absorbers', *Technical Papers Total Vehicle Dynamics*, Vol. 2, pp.117–120.

Li, H.J., Hu, S.J. and Takayama, T. (2000) 'Optimal tuned mass damper design for prolonging structural fatigue life', *Proceeding of the 8th ASCE Specialty Conference on Probabilistic Mechanics and Structural Reliability*, University of Notre Dame, Indiana, USA. Paper No. PCM2000-114.

Motta, D.S., Zampieri, D.E. and Pereia, A.K.A. (2000) 'Optimization of a vehicle suspension using a semi-active damper', *XI Congreso e Exposição Internacionais da Tecnologia da Mobilidade*, Outubro 3 a 5, São Paulo.

Scholz, P. (2000) μ-*MUSYCS User's Manual 2.0*, IMC GmbH, Berlin, Germany.

Singla, U.L. and Singh, S.P. (2004) 'Semi-active control of automotive vehicle suspension system using magnetorheological damper – a review', *SAE Technical Paper*, 2004-28-0077.

Yu, M., Liao, C.R., Chen, W.M. and Huang, S.L. (2006) 'Study on MR semi-active suspension system and its road holding', *Journal of Intelligent Material Systems and Structures*, Vol. 17, pp.801–806.